# Dielectric Spectroscopy Investigation on the Interaction of Poly(diallyldimethylammonium chloride) with Sodium Decyl Sulfate in Aqueous Solution

Zhen Chen,[†] Xin-Wei Li,[†] Kong-Shuang Zhao,*,[†] Jin-Xin Xiao,[‡] and Li-Kun Yang[†]

[†]College of Chemistry, Beijing Normal University, Beijing 100875, People's Republic of China
[‡]Beijing FLUOBON Surfactant Institute, Beijing 100080, People's Republic of China

ABSTRACT: The interaction between poly(diallyldimethylammonium chloride) (PDADMAC) and ionic surfactant sodium decyl sulfate ($C_{10}SO_4Na$) in aqueous solution was investigated by means of dielectric relaxation spectroscopy. To better understand the interaction, the dielectric behaviors of PDADMAC solution and $C_{10}SO_4Na$ solution were also separately studied. For PDADMAC solution, two relaxations were observed, which were attributed to the polarization of loosely bound counterions along the directions parallel and perpendicular to the PDADMAC chain. For $C_{10}SO_4Na$ solution, dielectric relaxation was observed at submicellar concentrations, which is ascribed to the counterion diffusion around premicelles. For the aqueous solutions of a PDADMAC/$C_{10}SO_4Na$ mixture with different $C_{10}SO_4Na$ concentrations, three surfactant concentration regions characterized by different dielectric behaviors were observed. The dielectric behavior in different regions was discussed through comparing it with that of PDADMAC solution and $C_{10}SO_4Na$ solution. The

possible interaction pattern and microstructure of the PDADMAC/$C_{10}SO_4Na$ complex were proposed on the basis of the dielectric behavior.
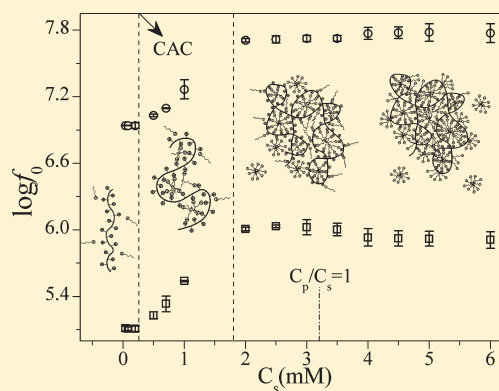
1. INTRODUCTION

The complexes formed by a polyelectrolyte and an oppositely charged surfactant have been widely applied in many industrial areas such as food, cosmetics, paints, and detergents and thus have attracted great interest in scientific research for many decades.[1-7] In this regard, the interaction between the oppositely charged polyelectrolyte and surfactant is always one of the most important research focuses. This interaction is much stronger and more complicated as compared with that between a neutral polymer and surfactant, because a strong electrostatic force is involved in addition to a relatively weaker hydrophobic force. It is well-known that the association of the surfactant with the polyelectrolyte starts from a critical association concentration (cac) that is generally 1 or 2 orders lower than the critical micelle concentration (cmc) of the pure surfactant solution. The mechanism of the association is commonly accepted as a cooperative binding process where many effects are involved, e.g., hydrophobic interaction between surfactant molecules, polyion charge neutralization, and conformational changes of the polyelectrolyte.[3] Therefore, many factors can influence this process, including the molecular weight, chain stiffness, charge density, and concentration of the polyelectrolyte, the chemical nature of different parts and concentration of the surfactant, and even the sequence of mixing the components.[7] Although great progress has been made in understanding the mechanism of this interaction, a lot of research has still been carried out recently,[8-18] trying to give a fuller perspective on the

interaction mechanism or related phenomenon from a new angle of views or new systems.

The interaction process is usually accompanied by changes in various physicochemical properties such as viscosity and surface tension.[1,2] Characterization of these properties is able to offer valuable information on the interaction mechanism and the structure of the polyelectrolyte–surfactant complex. To this end, a large number of characterization methods, for example, surface tension, dialysis equilibrium, NMR, and light and neutron scattering, have been employed.[19] Among these properties, however, the dielectric properties have for a long time been overlooked. The dielectric properties of a matter are essentially related to the fluctuation of the dipole moments and the motions of charges, characterization of which is therefore able to provide important, sometimes unique, information on the charge distribution and displacement, dynamics and structure of the dipole moment, intermolecular interactions, and so on.[20] As the suitable method to characterize the dielectric properties, dielectric relaxation spectroscopy (DRS) is now known as an effective modern method used in physical and chemical analyses of all kinds of materials.[20] This method has been applied to some polymer–surfactant systems such as solid polyelectrolyte–surfactant

complexes,[21] polyelectrolyte—lipid membranes,[22] and PVP—micelle aqueous solutions.[23] However, DRS study on the aqueous mixture solutions of a synthetic polyelectrolyte and an oppositely charged surfactant has rarely been reported as yet. On the other hand, DRS has been extensively applied to aqueous polyelectrolyte solutions for decades, successfully revealing the charge distribution and polyelectrolyte structure on the basis of the dielectric relaxations at different frequency ranges.[24−33] Also, surfactant solutions have been systematically characterized by this method.[34−36] Due to the maturity of DRS characterization of these systems, we believe it is worth carrying out DRS study on polyelectrolyte—surfactant mixture solutions, which may shed some light on the interaction mechanism from a particular angle of view.

This study is concerned with the interaction between a positively charged polyelectrolyte, poly(diallyldimethylammonium chloride) (PDADMAC), and a negatively charged surfactant, sodium decyl sulfate ($C_{10}SO_4Na$), in aqueous solution. PDADMAC is a water-soluble polyelectrolyte with a length of a monomer unit of about 0.54 nm, and it possesses the appropriate charge density and stretches in low concentration solution; it therefore has been widely applied in industry.[37,38] This polyelectrolyte is also broadly used for research on the polyelectrolyte—surfactant interaction, where sodium dodecyl sulfate (SDS) is the most frequently employed counterpart surfactant.[8,11,12,16,17] While most such investigations focus on the case of high surfactant concentration, we focus here on the polyelectrolyte—surfactant interaction under the condition that the surfactant concentration is much lower than the cmc, which in our opinion may lead to important consequences in the complexation process in the higher surfactant concentration range. Therefore, we choose $C_{10}SO_4Na$ as the counterpart surfactant instead, which is less hydrophobic than SDS and has a much higher cmc.[39,40] To better understand the dielectric behavior of this mixture solution, the dielectric behaviors of individual aqueous solutions of PDMDAAC and $C_{10}SO_4Na$ were also investigated for comparison.

2. EXPERIMENTAL SECTION

2.1. Materials. Sodium decyl sulfate, analytical grade, was provided by Beijing Chemical Plant and used without further purification. Aqueous solution of PDADMAC (average molecular weight 200000−350000) with a weight fraction of 20% was purchased from Aldrich. Highly deionized water was obtained from the Aquapro P series water purification system (Taiwan).

2.2. Sample Preparation. Aqueous solutions of $C_{10}SO_4Na$ with different concentrations (0.04−100 mM) were prepared by dissolving a certain amount of $C_{10}SO_4Na$ in highly deionized water. Aqueous solutions of PDADMAC with weight fractions of 0.05%, 0.1%, 0.3%, 0.5%, and 1.0% were prepared by diluting 20% PDADMAC solution with deionized water. To obtain homogeneous solutions, all PDADMAC solutions were left to equilibrate for 12 h prior to dielectric measurement. Aqueous solutions of the PDADMAC/$C_{10}SO_4Na$ mixture were prepared by adding $C_{10}SO_4Na$ into 0.05% PDADMAC aqueous solutions. In these mixture solutions, the weight fraction of PDADMAC was kept at 0.05% while the concentration of $C_{10}SO_4Na$ (C_s) was varied from 0.04 to 6.0 mM. When $C_s < 2$ mM, the mixture solutions were transparent. When $C_s \geq 2$ mM, a cloudy solution was observed right after $C_{10}SO_4Na$ was added. For the sake of complete dissolution and equilibrium, all mixture solutions were kept for over 80 h before testing. Even though, a white curdy precipitation was observed for mixture solutions with

$C_s \geq 2.5$ mM. In these cases, the supernate of the samples was used for dielectric measurement.

2.3. Dielectric Measurement. Dielectric measurements were carried out on an HP 4294A precision impedance analyzer (Agilent Technologies) which covers a frequency range from 40 Hz to 110 MHz. A dielectric cell with concentrically cylindrical platinum electrodes[41] was employed to load the samples. All the experimental data were corrected for errors arising from stray capacitance (C_r) and the cell constant (C_l).[42] They are 0.0265 and 0.474 pF, respectively, determined with water, ethanol, and air. The measurements directly obtained the capacitance (C) and conductance (G) of the samples. Then the relative permittivity (ε) and conductivity (κ) were determined by $C = \varepsilon C_l + C_r$ and $G = \kappa C/\varepsilon\varepsilon_0$, where ε_0 is the permittivity of a vacuum. All dielectric measurements were carried out at 25 ± 1 °C.

2.4. Determination of Dielectric Parameters. The dielectric property of a material is generally characterized in terms of the complex permittivity ε^* defined as

$$\varepsilon^* = \varepsilon - j\varepsilon'' = \varepsilon - j\frac{\kappa - \kappa_{dc}}{\omega\varepsilon_0} \qquad (1)$$

where ε is the relative permittivity, ε'' is the dielectric loss, κ is the conductivity, κ_{dc} is the dc conductivity, ω (=$2\pi f$) is the angular frequency, and $j^2 = -1$. In our investigated frequency window, one or two relaxations were observed, and because the samples are conductive, there exists a considerable electrode polarization (EP) effect due to the accumulation of spatial charge at the electrode—solution interface. Accordingly, the following relaxation function was employed to analyze the experimental spectra:[20,29,32,33]

$$\varepsilon^* = \varepsilon_h + \sum_i \frac{\Delta\varepsilon_i}{1 + (j\omega\tau_i)^{\beta_i}} + A\omega^{-m} \qquad (2)$$

where ε_h is the high-frequency limit of the relative permittivity. The second term of the right-hand side in eq 2 is the Cole—Cole relaxation function accounting for the contribution from effective relaxation mechanisms, where i is the number of dielectric relaxations, $\Delta\varepsilon_i$ is the dielectric increment, τ_i (=$1/(2\pi f_{0i})$; f_{0i} is the characteristic relaxation frequency) is the relaxation time of the ith dielectric relaxation, and β_i ($0 < \beta_i \leq 1$) is the Cole—Cole parameter indicating the distribution of the relaxation time. The third term takes into account the EP effect on the basis of the power-law frequency dependence method,[41] where A and m are adjustable parameters.

Meanwhile, the logarithmic derivative (LD) method[43,44] was used to optimize the fitting, which is based on the following derivative:

$$\varepsilon''_{LD}(\omega) = -\frac{\pi}{2}\frac{\partial\varepsilon}{\partial\ln\omega} \approx \varepsilon''_{Rel}(\omega) \qquad (3)$$

where ε''_{LD} and ε''_{Rel} denote the derivative dielectric loss and the dielectric loss free of dc conductivity, respectively. This method is effective in separating relaxations from the EP effect and also offers a good way to resolve overlapping relaxation peaks due to peak sharpening.[44] As a representative case, Figure 1 shows the frequency dependence of the relative permittivity (inset) and its derivative dielectric loss of 0.05% PDADMAC aqueous solution. As can be clearly seen, although only one relaxation is observed in the ε spectrum, two relaxations can be observed in the ε''_{LD} spectrum.

5767

dx.doi.org/10.1021/jp200486u |*J. Phys. Chem. B* 2011, 115, 5766–5774
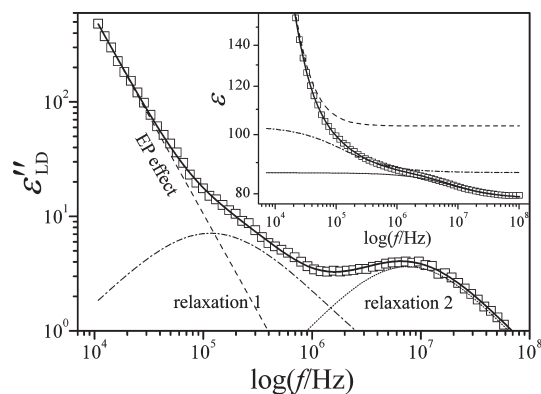
Figure 1. Frequency dependence of the derivative dielectric loss of 0.05% PDADMAC aqueous solution: solid line, best fit; dashed line, EP effect; dashed−dotted line, lower frequency relaxation; short dotted line, higher frequency relaxation. The inset shows the fitting result of the relative permittivity by using the same fitting parameters.

By introducing the real part of eq 2 into the derivative expression (eq 3), we get the following expression:

$$\varepsilon''_{LD} = \frac{\pi}{2}\left(\sum_i \frac{\beta_i \Delta\varepsilon_i (\omega\tau_i)^{\beta_i} \cos[\beta_i \pi/2 - (1+\beta_i)\theta_i]}{1 + 2(\omega\tau_i)^{\beta_i} \cos(\beta_i \pi/2) + (\omega\tau_i)^{2\beta_i}} + Am\omega^{-m}\right) \tag{4}$$

where $\theta_i = \arctan[\sin(\beta_i\pi/2)/((\omega\tau_i)^{-\beta_i} + \cos(\beta_i\pi/2))]$. This equation has the same set of variables as that in eq 2 and can be used to fit the derivative dielectric loss curve. The solid line in the ε''_{LD} spectrum in Figure 1 represents the best fit in line with eq 4, which is a superposition of the EP effect and the contributions from the lower and higher frequency relaxations (relaxation 1 and relaxation 2, respectively, hereinafter). The solid line in the ε spectrum (inset of Figure 1) is the calculated curve in line with eq 2 by using the same parameters as in ε''_{LD} curve fitting, which agrees perfectly with the experimental curve. In fact, a good fitting on the ε''_{LD} curve always results in a good agreement between the calculated curve and the experimental ε curve, because ε''_{LD} is equivalent to ε through eq 3. Also because of this, we cannot determine the relaxation parameters by only fitting the ε''_{LD} curve and/or its equivalent ε curve, and we must at the same time take the imaginary part of complex permittivity (conductivity) into account.

According to eqs 2 and 4, up to nine variables, including ε_h (or κ_{dc}), $\Delta\varepsilon_1$, $\Delta\varepsilon_2$, f_{01}, f_{02}, β_1, β_2, A, and m, are involved in the curve fitting for a two-relaxation profile. With so many variables, it is generally difficult to determine these dielectric parameters with high reliability. Nevertheless, it should be pointed out that because the values of f_{01}, f_{02}, and ε_h (κ_{dc}) can be determined directly from the spectra, the actual number of fitting variables is reduced to 6, which greatly improves the reliability of the fitting. The values of f_{01} and f_{02} can be directly read from the ε''_{LD} curve because in most cases relaxations 1 and 2 are well separated from each other and the EP effect is largely reduced by using the LD method (see Figure 1). Since the high-frequency tail of relaxation 2 in most cases is visible, the value of ε_h can be read from the ε curve, which approximates the value of the relative permittivity at the high-frequency end. The value of κ_{dc} can be read from the κ curve, which corresponds to the value of conductivity at the low-frequency limit (see Figure 2).
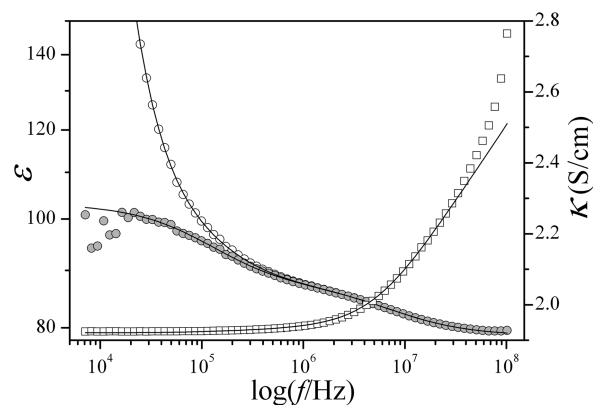

Figure 2. Frequency dependence of the relative permittivity and conductivity of 0.05% PDADMAC aqueous solution. Filled circles are the relative permittivity after subtraction of the EP effect, and the solid lines represent the best fits.

To ensure the fitting result is more reliable, a multistep fitting procedure was followed. Figure 2 shows a representative fitting result in this way. First, a preliminary simultaneous fit of the ε curve and ε''_{LD} curve was made, by which the values of A and m were roughly determined. The optimized fitting result was guaranteed by the nonlinear least-squares method. The EP effect was then subtracted from the ε curve by using the parameters A and m, and a new ε curve free of EP effect was derived (the filled circle curve in Figure 2). Next, a simultaneous fit of the new ε curve and the κ curve was made, where the actual number of variables is reduced to 4. Also, the nonlinear least-squares method was used to minimize the sum of the residuals between them. Finally, the new set of parameters thus obtained was used to simultaneously fit the original ε curve and ε''_{LD} curve again to optimize the parameters A and m. This multistep procedure was repeated until these parameters converged to stable values. As an example, for the case of 0.05% PDADMAC solution the set of parameters derived in this way is $\Delta\varepsilon_1 = 17.23 \pm 0.13$, $\Delta\varepsilon_2 = 8.06 \pm 0.09$, $f_{01} = 120.16 \pm 9.25$ kHz, $f_{02} = 7.58 \pm 0.25$ MHz, $\beta_1 = 0.75 \pm 0.01$, $\beta_2 = 0.77 \pm 0.01$, and $\varepsilon_h = 78.56 \pm 1.28$. The values of β_1 and β_2 are typical for aqueous solutions of polyelectrolyte.[24,28,30] They are smaller than unity, indicating that the distribution of the relaxation time exists for both the relaxations. This is mainly ascribed to the distribution of the molecular weight of PDADMAC molecules. The value of ε_h is very close to the value of the static relative permittivity of pure water (78.54 at 25 °C). Furthermore, the dielectric relaxations due to the dynamics of water molecules generally occur in a much higher frequency range (GHz). These facts suggest that the dynamics of water molecules is not involved in the dielectric relaxations under consideration. Similar results were also found for other samples; therefore, the dynamics of water molecules will not be considered in our discussion.

3. RESULTS AND DISCUSSION

3.1. Dielectric Behavior of PDMDAAC Aqueous Solutions. Aqueous solutions of polyelectrolyte have been extensively investigated by DRS for decades.[24−33] In the frequency range investigated, two dielectric relaxations can be expected in the frequency ranges of 10−100 kHz and 1−100 MHz, which are generally called low-frequency (LF) relaxation and intermediate-frequency (IF) relaxation, respectively.[29]
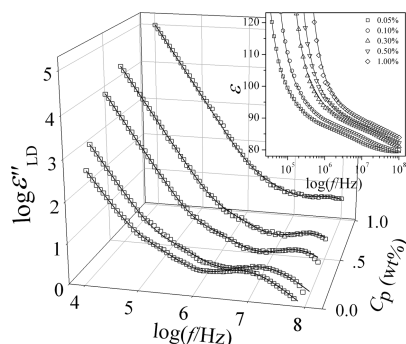
Figure 3. Three-dimensional plot of the derivative dielectric loss of PDADMAC aqueous solution as functions of the frequency and polyelectrolyte concentration. The inset shows the frequency dependence of the relative permittivity of the solutions with different concentrations. The solid lines are the best fits.

The LF relaxation is much less investigated than the IF relaxation, because it is often seriously covered by the EP effect. The study on NaPSS[24−26] and xanthan[28] solutions indicated that this relaxation is characterized by an increasing $\Delta\varepsilon$ and a relatively constant τ_0 with increasing polyelectrolyte concentration (for dilute and semidilute solution). Therefore, this relaxation is thought to be ascribed to the polarization of condensed (tightly bound) counterions along the polymer chain that is essentially stationary on this time scale.[29]

Although extensively investigated, the mechanism of the IF relaxation is still under controversy. Three classes of ideas have been presented to account for it, among which the scaling law proposed by Ito et al.[27,29] has been extensively employed in recent investigations. They attributed this relaxation to the fluctuation of loosely bound counterions on the scale of the correlation length ξ. The relaxation time hence corresponds to the time of the counterions diffusing at a length scale of ξ and is given by

$$\tau_0 \approx \xi^2/2D \propto \xi^2 \tag{5}$$

where D is the diffusion coefficient of the counterions. For semidilute solution without salt, ξ is given by $\xi \approx C_p^{-1/2}N^0$, where the superscript stands for the exponent, C_p is the concentration of polyelectrolyte, and N is the degree of polymerization. Therefore, τ_0 has the following scaling relationship:[27,29]

$$\tau_0 \propto C_p^{-1}N^0 \tag{6}$$

On the other hand, $\Delta\varepsilon$ is decided by the number concentration n_L and the electrical polarizability α_e of loosely bound counterions as $\Delta\varepsilon = n_L\alpha_e/\varepsilon_0$.[25] The electrical polarizability of loosely bound counterions is decided by their charge e and polarization distance ξ:

$$\alpha_e \approx e^2\xi^2/kT \approx e^2N^0/C_p^{1/2}kT \tag{7}$$

where k and T are the Boltzmann constant and absolute temperature, respectively. Meanwhile, n_L is proportional to C_p but independent of N. Therefore, $\Delta\varepsilon$ has the following scaling relationship:[27,29]

$$\Delta\varepsilon \propto C_p^0N^0 \tag{8}$$

In the present case, since the concentrations of PDADMAC solutions are higher than the crossover concentration (0.024%, determined by experiment[33]), they are at least semidilute solutions.
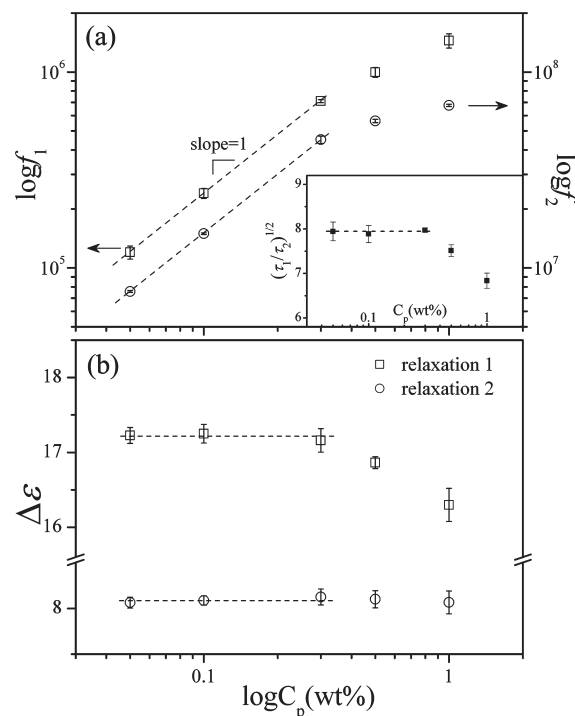

Figure 4. Relaxation frequency (a) and dielectric increment (b) of PDADMAC solutions as a function of the polymer concentration. The dashed lines are drawn for guiding the eye. The inset in (a) shows the concentration dependence of $(\tau_1/\tau_2)^{1/2}$.

The typical dielectric behavior has been shown in Figures 1 and 2, and the observed relaxation 1 and relaxation 2 should correspond to the LF and IF relaxations, respectively. The dielectric spectra of the derivative dielectric loss and relative permittivity of PDADMAC aqueous solutions with different C_p values are shown in Figure 3. Two relaxations can be observed for all samples, both shifting to the higher frequency range with increasing C_p.

According to the fitting results, the values of β_1 and β_2 for all solutions are independent of C_p. The C_p dependences of f_0 and $\Delta\varepsilon$ of these PDADMAC solutions are summarized in parts a and b, respectively, of Figure 4, where a clear break shows up at $C_p \approx 0.3\%$. When $C_p \leq 0.3\%$, the dielectric behavior of relaxation 2 is consistent with the scaling law for semidilute solution: $\Delta\varepsilon$ is nearly constant, while f_0 is perfectly proportional to C_p with a slope of unity. It is interesting that the variation of f_0 and $\Delta\varepsilon$ of relaxation 1 has the same tendency as that of relaxation 2. This result is different from the cases observed in other electrolyte solutions such as NaPSS.[26] In addition, f_0 of relaxation 1 in this case is much higher than that of other polyelectrolytes with comparable chain size. Therefore, we doubt that relaxation 1 in this case is ascribed to the fluctuation of tightly bound counterions along the polymer chain. Instead, because of the same variation tendency as relaxation 1, we believe this relaxation has an origin similar to that of relaxation 2, namely, the fluctuation of loosely bound counterions on the order of ξ.

Considering the linear configuration of PDADMAC molecules, relaxations 1 and 2 are possibly due to the fluctuation of loosely bound counterions along the directions parallel and perpendicular to the polymer chain, respectively. It should be noted that the effective persistence length of linear polyelectrolyte molecules is also on the order of the correlation length,
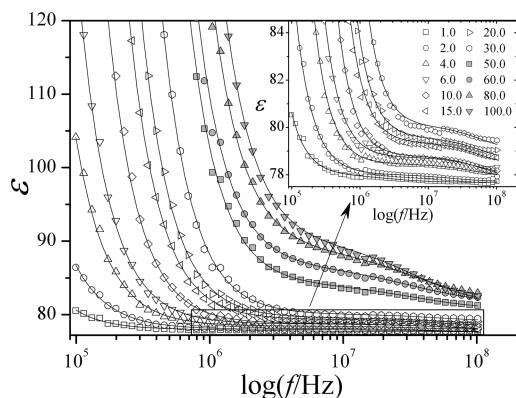
5769

dx.doi.org/10.1021/jp200486u |*J. Phys. Chem. B* 2011, 115, 5766–5774

Figure 5. Frequency dependence of the relative permittivity of $C_{10}SO_4Na$ aqueous solutions with different surfactant concentrations. The solid lines represent the best fits.
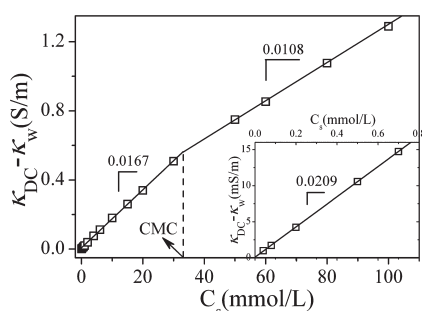

Figure 6. Effective conductivity of $C_{10}SO_4Na$ aqueous solutions as a function of the surfactant concentration. The inset is an enlargement of solutions with concentration lower than 1 mM.
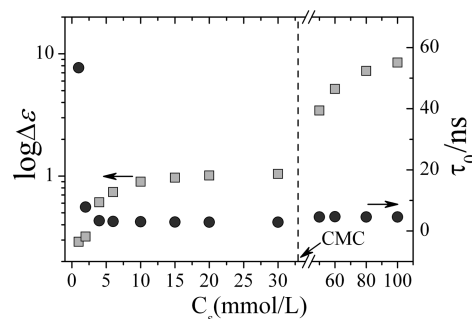

Figure 7. Relaxation time (filled circles) and dielectric increment (filled squares) of $C_{10}SO_4Na$ aqueous solutions as a function of the surfactant concentration.

because the polyelectrolyte chain in the semidilute solution is a random walk of correlation blobs.[45] If this is the case, we can compare the characteristic lengths parallel and perpendicular to the polymer chain through $(\tau_1/\tau_2)^{1/2}$ according to eq 5. The inset in Figure 4a shows the result, from which we can see the parallel characteristic length is about 1 order larger than the perpendicular one. When $C_p \leq 0.3\%$ the ratio between the characteristic lengths remains constant (about 7.92), suggesting the local configuration of PDADMAC molecules barely changes in this concentration range.

When $C_p > 0.3\%$, f_0 of both relaxations becomes less dependent on C_p, and $\Delta\varepsilon$ of relaxation 1 decreases obviously. This suggests that the solution may go to the entangled semidilute or concentrated region. However, because of the lack of experimental data and the larger experimental error due to approaching the high-frequency limit, any further discussion in this concentration range is arbitrary.

3.2. Dielectric Behavior of Surfactant Aqueous Solutions. While dielectric measurement was performed on all prepared $C_{10}SO_4Na$ solutions, no relaxation was observed for solutions with surfactant concentration (C_s) lower than 1 mM. For solutions with $C_s \geq 1$ mM, only one relaxation was observed in the investigated frequency range, as shown in Figure 5. It is worth noting that, although the cmc of $C_{10}SO_4Na$ is about 33 mM,[39,40] dielectric relaxation is also observed for solutions with $C_s <$ cmc, which suggests that premicelles are formed below the cmc. The formation of premicelles has been extensively reported both experimentally[46-48] and theoretically,[49,50] and in

some cases premicelles can be formed at a concentration more than 1 order lower than the cmc.[48]

Figure 6 shows the C_s dependence of the effective conductivity ($\kappa_{dc} - \kappa_W$) of the surfactant solutions. $\kappa_{dc} - \kappa_W$ is the difference between the dc conductivity of the surfactant solution κ_{dc} and that of water κ_W, which thus should be decided by

$$\kappa_{dc} - \kappa_W = fC_s(\lambda_s + \lambda_c^0) \qquad (9)$$

where f is the free counterion fraction, λ_s is the equivalent conductivity of the surfactant monomer, and λ_c^0 is the equivalent conductivity of the counterion in an infinitely dilute solution. As f barely changes, the slope of $\kappa_{dc} - \kappa_W$ vs C_s is mainly a function of λ_s and therefore reflects the aggregation state of surfactant monomers. From Figure 6 we can see there are three concentration regions characterized by different slopes (with a unit of $S \cdot m^2 \cdot mol^{-1}$). The low concentration region ($C_s < 1$ mM) has the largest slope, suggesting most surfactant molecules stay as monomers. When $C_s >$ cmc, the slope is obviously smaller than those of the other two regions. This should be a result of the formation of stable micelles, in which the surfactant monomers are much less movable. The slope in the intermediate concentration region (1 mM $< C_s <$ cmc) is systematically larger than that of the low concentration region, suggesting loose surfactant aggregates (premicelles) are formed.

The aggregation state is also reflected by their dielectric behavior. For solutions with $C_s < 1$ mM, because no aggregates are formed and the dielectric relaxation due to the rotation of the surfactant monomer generally occurs in much higher frequency range,[35] no relaxation can be observed in the investigated frequency range. For solutions with higher C_s, Figure 7 shows their C_s dependences of τ_0 and $\Delta\varepsilon$. As can be seen, a clear break characterized by a sudden increase of $\Delta\varepsilon$ shows up at the cmc, suggesting an essential change of aggregation state.

Above the cmc, the observed dielectric relaxation should be attributed to stable micelles. The value of β remains around 0.9, which is very close to 1. This suggests that the size of the micelles is nearly homogeneous. The dielectric response of stable micelles can be well described by the Grosse model:[34-36] a low-frequency relaxation due to the radial diffusion of the counterion at a distance on the order of the radius of the micelles and a high-frequency relaxation due to the tangential motion of bound counterions on the surface of micelles. According to this model, the low-frequency relaxation has a mean relaxation time on the order of a^2/D, where a and D are the radius of the micelle and the diffusion coefficient of the counterion, respectively. Therefore, the low-frequency relaxation time is mainly decided by the size of the micelle. The
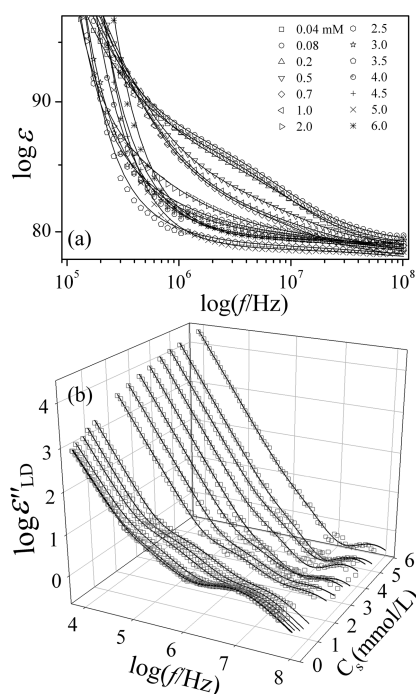
Figure 8. Frequency dependence of the relative permittivity (a) and derivative dielectric loss (b) of aqueous solutions of PDADMAC/C$_{10}$SO$_4$Na mixtures with different surfactant concentrations. The solid lines are the best fits.

Figure 9. Characteristic relaxation frequency (a) and dielectric increment (b) of both relaxations of PDADMAC/C$_{10}$SO$_4$Na mixture solutions as a function of the surfactant concentration. The arrows indicate the case of 0.05% PDADMAC solution, and the gray area denotes the precipitation zone.

high-frequency relaxation time corresponds to the time of bound counterions diffusing on the scale of the Debye length; it is therefore mainly a function of the solution conductivity.[34] Because κ_{dc} increases obviously with increasing C_s while the radius of stable micelles changes slightly, the nearly constant τ_0 definitely indicates that the observed relaxation is attributed to the radial diffusion of counterions.

For solutions with 1 mM < C_s < cmc, premicelles are supposed to be formed. The value of β is also around 0.9, suggesting the size of the premicelles is also homogeneous. The dielectric behavior of C$_8$TAB premicelles was investigated by DRS,[35] which is attributed to the fluctuation of the diffuse ion cloud around the aggregates, similar to that of stable micelles. Therefore, τ_0 of premicelles is also decided by their size, and $\Delta\varepsilon$ is mainly decided by the aggregation number, which is essentially proportional to the concentration of counterion in the diffuse ion cloud. When $C_s \leq 2$ mM, τ_0 decreases obviously with increasing C_s while $\Delta\varepsilon$ increases slightly. This seems to imply that the radius of the premicelles decreases obviously with increasing C_s while the aggregation number barely changes. When $C_s > 2$ mM, τ_0 is kept almost constant while $\Delta\varepsilon$ increases with C_s. This seems to indicate that more and more monomers are incorporated into the premicelles but their size remains almost unchanged. Interestingly, τ_0 in this concentration range is even smaller than that of stable micelle solutions, meaning that the radius of the premicelle is smaller than that of the stable micelle. This is possibly because a steric effect also plays a role in the formation of the premicelle and micelle.

3.3. Interaction between PDMDAAC and C$_{10}$SO$_4$Na in Aqueous Solution. *3.3.1. Dielectric Behavior of the Aqueous Solution of the PDADMAC/C$_{10}$SO$_4$Na Mixture.* Figure 8 shows the dielectric response of the aqueous solutions of the PDADMAC/C$_{10}$SO$_4$Na mixture with different surfactant concentrations (C_s),
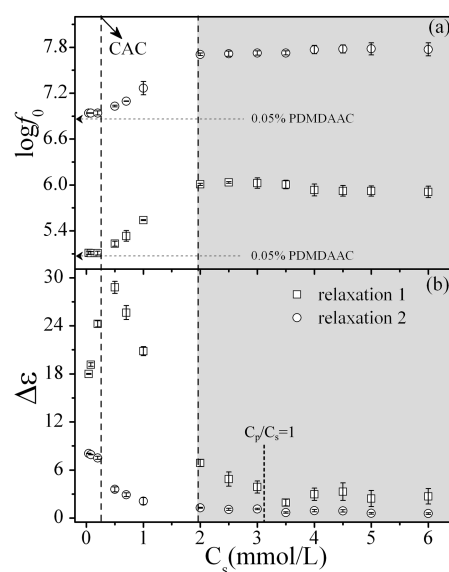
where parts a and b show the frequency dependence of the relative permittivity and derivative dielectric loss, respectively. C_s varies from 0.04 to 6 mM, which is far below the cmc, while the concentration of PDADMAC (C_p) is kept equal to 0.05 wt % (about 3.1×10^{-3} mmol/L). For simplification, we call these solutions PSI (polyelectrolyte−surfactant interaction) solutions hereinafter. As can be seen in Figure 8, two dielectric relaxations can also be observed for all PSI solutions, and both of them are sensitive to C_s.

Figure 9 shows the C_s dependence of f_0 and $\Delta\varepsilon$ of both relaxations of PSI solutions. Two breaks can be observed at $C_s \approx 0.25$ mM and $C_s \approx 2.0$ mM, which divide the surfactant concentration into three regions.

In the low concentration region (C_s < 0.25 mM), the dielectric spectra of PSI solutions are quite similar to that of 0.05% PDADMAC solution, with comparable β, f_0, and $\Delta\varepsilon$ for both relaxations 1 and 2. Both relaxations thus should have the same origins as those of PDADMAC solution. With a closer look at the results, we find the f_0 values of both relaxations are barely changed with surfactant concentration but their values are slightly higher than that of 0.05% PDADMAC solution, which suggests that the parallel and perpendicular characteristic lengths are smaller in the presence of surfactant. $(\tau_1/\tau_2)^{1/2}$ is calculated to be 8.22, 8.25, and 8.36 for PSI solutions with 0.04, 0.08, and 0.2 mM surfactant, respectively. These values are systematically bigger than that of 0.05% PDADMAC solution, suggesting the polymer chain in the presence of surfactant is more "stretched"; namely, the parallel characteristic length shrinks less intensely than the perpendicular one. On the other hand, we noticed that $\Delta\varepsilon_1$ increases obviously while $\Delta\varepsilon_2$ decreases slightly with increasing C_s. Note that $\Delta\varepsilon$ is not only a function of the characteristic length but also a function of the number concentration of loosely bound counterion n_L (see section 3.1); the increasing $\Delta\varepsilon_1$ thus suggests that n_L increases with increasing C_s. For $\Delta\varepsilon_2$, its decrease with increasing C_s is probably because the increasing n_L is not enough to compensate for the effect of the
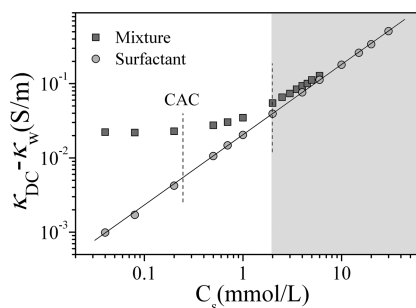
Figure 10. Effective conductivity of $C_{10}SO_4Na$ solution (filled circles) and of PDADMAC/$C_{10}SO_4Na$ mixture solutions (filled squares) as a function of the surfactant concentration. The solid line is drawn for guiding the eyes, and the gray area denotes the precipitation zone.

decrease in characteristic length. Because the association of surfactant monomer with PDADMAC will neutralize the polymer chain and thus decrease the concentration of counterion, the increasing n_L with increasing C_s strongly suggests there is no association between them in this concentration region. As a result, the PDADMAC molecule acts like a buffer and the addition of surfactant will condense the counterion cloud of PDADMAC molecules, similar to the addition of added salt,[51] which will drive more free counterions into the loosely bound area. On the other hand, the conductivity of the whole PSI solution should be nearly unchanged.

The C_s dependences of $\kappa_{dc} - \kappa_W$ of PSI solutions and $C_{10}SO_4Na$ solutions are compared in Figure 10. Two clear breaks can also be seen in the case of PSI solutions, and the transition concentrations are consistent with those observed in Figure 9.

In the low concentration region ($C_s = 0.25$ mM), $\kappa_{dc} - \kappa_W$ of PSI solution is barely changed with increasing C_s. This result supports the interpretation above; that is, no obvious association between surfactant monomer and polyelectrolyte occurs, and the PDADMAC molecule acts like a buffer.

In the intermediate concentration region (0.25 mM < C_s < 2.0 mM), f_0 of both relaxations increases; meanwhile $\Delta\varepsilon$ decreases noticeably as C_s increases. The condensation of the counterion cloud like the case in the low concentration region cannot give rise to such a remarkable change; therefore, the results suggest the association of surfactant molecules with the polymer chain. Due to the association, the polymer chain is partially neutralized and thus locally collapses, resulting in a smaller characteristic length. Meanwhile, the n_L inside the correlation volume also decreases with the neutralization of the polymer chain, so $\Delta\varepsilon$ decreases with increasing C_s. It is noteworthy that $\Delta\varepsilon_1$ is still bigger than that of pure PDADMAC solution. Since the concentration of tightly bound counterions of these solutions should be largely reduced because of surfactant association, this result is evidence that relaxation 1 is attributed to the fluctuation of loosely bound counterions rather than tightly bound counterions. The values of $(\tau_1/\tau_2)^{1/2}$ for PSI solutions with 0.5, 0.7, and 1.0 mM surfactant are calculated to be 8.03, 7.57, and 6.69, respectively. These values decrease with increasing C_s, suggesting that the polymer chain is more and more "coiled" due to the surfactant association. In the same concentration region, $\kappa_{dc} - \kappa_W$ of PSI solution increases with C_s as shown in Figure 9, even though the slope of $\kappa_{dc} - \kappa_W$ vs C_s is smaller than that of pure surfactant solution. This also indicates

the association of surfactant with the polymer chain, considering that the bound surfactant monomers are less movable than those in bulk solution. Accordingly, the transition concentration (about 0.25 mM) between these two concentration regions should correspond to the cac, which is about 2 orders of magnitude lower than the cmc of $C_{10}SO_4Na$.

The high concentration region (2.0 mM < C_s < 6 mM) is in the vicinity of the charge neutralization point ($C_p/C_s = 1$). During the sample preparation, it was observed that a cloud shows up in the PSI solution in this concentration region. After full dissolution and equilibrium for 80 h, the solution with $C_s = 2.0$ mM turned back to transparent, indicating the PSI process is time-consuming. For other PSI solutions, the curdy precipitate was still observed. This concentration region thus can be thought of as the precipitation region. It should be pointed out that only the supernate of the samples in this concentration range (except for the 2.0 mM case) was dielectrically measured, in which most polyelectrolyte—surfactant complexes have precipitated out. Nevertheless, we can find that the dielectric behavior of the supernate of PSI solutions is much different from that of pure surfactant solutions: two relaxations are still observed. Therefore, considerable complexes should still exist in the supernate, which might be dispersed as colloids.

As shown in Figure 10, $\kappa_{dc} - \kappa_W$ of PSI solution increases with increasing C_s with a slope nearly consistent with that of pure surfactant solution, which seems to imply that surfactant aggregates play an important role in the dielectric and conductance behavior in this concentration region. From Figure 9 we can see that both f_{02} and $\Delta\varepsilon_2$ have magnitudes comparable to those of surfactant solutions. In addition, while the value of β_2 in the low and intermediate concentration regions remains around 0.77, it is increased to around 0.9 in this region, which is also comparable to that of surfactant solution. On the other hand, since most charged sites on the polymer chain are neutralized, which means few counterions are present, relaxation 2 cannot be attributed to the fluctuation of loosely bound counterions. According to these facts, relaxation 2 is very likely ascribed to the polarization of surfactant aggregates. We noticed that although the actual surfactant concentration in the supernate should be much lower than the overall surfactant concentration (C_s) of its mother solution, the value of $\Delta\varepsilon_2$ is still larger than that of pure surfactant solution with the same C_s (see Figure 7). Therefore, we believe relaxation 2 is mainly attributed to the surfactant aggregates on the polymer chain. These aggregates are either trapped by the polymer chain or restrained on the surface of the polyelectrolyte—surfactant complex. The contribution of free premicelle to this relaxation cannot be excluded, considering that the local surfactant concentration might be high in the presence of complexes[7] and that $C_{10}SO_4Na$ easily forms premicelles at even low concentration.

Relaxation 1 must be closely related to the polyelectrolyte—surfactant complex, because this relaxation is absent from pure surfactant solutions. Considering that the complexes are dispersed as colloids which may have a size on the scale of nanometers, relaxation 1 is most likely due to either the polarization of the counterion cloud around the complexes or the interfacial polarization effect, as observed in many colloidal dispersions.[52,53] Whatever the case is, $\Delta\varepsilon_1$ should be scaled with the concentration of the complexes in the supernate. The value of β_1 is around 0.8 in this concentration region, which suggests that the complexes have a narrow distribution in size. We noticed that the variation of $\Delta\varepsilon_1$ vs C_s reaches a minimum at
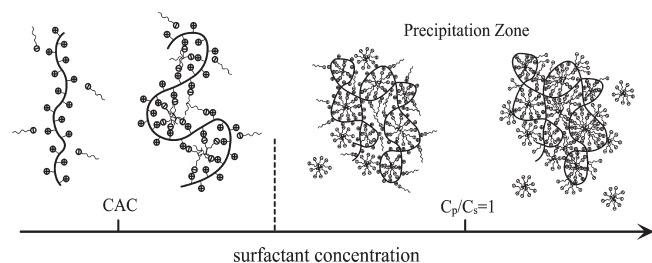
Figure 11. Schematic illustration of the possible interaction pattern between PDADMAC and $C_{10}SO_4Na$ in aqueous solution with low $C_{10}SO_4Na$ concentrations.

$C_s \approx 3.5$ mM, a little higher than the charge neutralization point. This concentration seems to divide the precipitation region into two subregions. Below this concentration, the decreasing $\Delta\varepsilon_1$ with increasing C_s suggests that the concentration of dispersed complexes decreases with increasing C_s. This is because the polyelectrolyte chain is not completely neutralized by surfactant; the addition of surfactant will further neutralize the complexes and then lead to the precipitation of more complexes. Above this concentration, surfactant monomers will still be absorbed on the surface of the complexes due to hydrophobic interaction, which dissolves some complexes. Therefore, the concentration of the complexes should be increased with the addition of surfactant, resulting in an increasing $\Delta\varepsilon_1$.

3.3.2. Possible Interaction Pattern and Microstructure in PSI Solutions. According to the dielectric and conductance behavior of PSI solutions, the possible interaction process and the possible microstructure of the polyelectrolyte–surfactant complex in bulk solution with the addition of $C_{10}SO_4Na$ may be like those schematically illustrated in Figure 11.

When C_s is smaller than the cac, no obvious association between surfactant and polymer chain occurs, and the PDADMAC chain is more stretched than in pure polymer solution. The surfactant molecules stay as monomers and act as added salt. As a result, the counterion cloud of polyelectrolyte is condensed due to the presence of surfactant, which then gives rise to a higher concentration of loosely bound counterion and smaller characteristic length.

When cac < C_s < 2 mM, surfactant monomers start to associate with the charge sites on the polymer chain, and small surfactant aggregates are formed. Since part of the charge sites are neutralized, the polymer chain starts to self-contract. However, the polymer chain is still locally stretched, and self-entanglement is forbidden because considerable electrostatic repulsion still remains. When C_s > 2 mM, the polymer chain is further neutralized, and hydrophobic attraction starts to become dominant. Globular complexes as shown in Figure 11 might be formed. While most complexes congregate and then precipitate, some isolated complexes are still present as colloids in the bulk solution. In the concentration subregion below the charge neutralization point, since some charge sites on the polymer chain still remain unneutralized, the complex as a whole is positively charged. When C_s is bigger than the charge neutralization point, some precipitated complexes are redissolved because of the adsorption of excess surfactants as a result of hydrophobic interaction, which as a whole are negatively charged. The charges that the colloidal complexes bear in the precipitation zone prevent them from precipitation.

4. CONCLUSION

The interaction between PDADMAC and $C_{10}SO_4Na$ in aqueous solutions was investigated by means of DRS, on the basis of the understanding of the dielectric behaviors of their individual component aqueous solutions.

It was found that DRS is effective in characterizing the interaction between oppositely charged polyelectrolyte and surfactant in aqueous solution. The cac can be conveniently confirmed by the dielectric and conductive behavior of the system. No obvious association of surfactant with polyelectrolyte is observed below the cac, but we found that the polyelectrolyte chain is more stretched than in pure polymer solution. This is attributed to the counterion condensation of polyelectrolyte as a result of the presence of surfactant monomers. Above the cac, we found that there exists a preprecipitation concentration range in which the association of surfactant with polyelectrolyte cannot devastatingly change the local configuration of the polymer chain. In the precipitation concentration range, it was found that considerable polyelectrolyte—surfactant complexes are still dissolved in bulk solution. The dielectric behavior suggested that these colloidal complexes bear charges, either due to incomplete neutralization or because of the absorption of excess surfactant.

While DRS measurement can cover a frequency range of more than 12 orders, the present study is limited to just a narrow frequency window. If a higher frequency range is covered, much more information can be obtained, such as the state of surfactant monomers and the dynamics of water molecules.[29,35,36] Since the information obtained in different frequency ranges is complementary to each other, deeper insight into the interaction mechanism by means of DRS is worthy of expectation.

■ AUTHOR INFORMATION

Corresponding Author
*Phone: +861058808283. E-mail: zhaoks@bnu.edu.cn.

■ ACKNOWLEDGMENT

■ REFERENCES

(1) Goddard, E. D. Polymer—Surfactant Interaction Part II: Polymer and Surfactant of Opposite Charge. In *Interaction of Surfactants with Polymers and Proteins*; Goddard, E. D., Ananthapadmanabhan, K. P., Eds.; CRC Press: Boca Raton, FL, 1993; pp 171—202.

(2) Kwak, J. C. T. *Polymer—Surfactant Systems*; Marcel Dekker: New York, 1998.

(3) Wei, Y. C.; Hudson, S. M. *J. Macromol. Sci., Rev. Macromol. Chem. Phys.* **1995**, *C35*, 15–45.

(4) Piculell, L.; Guilemet, F.; Thuresson, K.; Shubin, V.; Ericsson, O. *Adv. Colloid Interface Sci.* **1996**, *63*, 1–21.

(5) Iliopoulos, I. *Curr. Opin. Colloid Interface Sci.* **1998**, *3*, 493–498.

(6) Mesa, C. L. *J. Colloid Interface Sci.* **2005**, *286*, 148–157.

(7) Langevin, D. *Adv. Colloid Interface Sci.* **2009**, *147—148*, 170–177.

(8) Staples, E.; Tucker, I.; Penfold, J.; Warren, N.; Thomas, R. K.; Taylor, D. J. F. *Langmuir* **2002**, *18*, 5147–5153.

(9) Wang, C.; Tam, K. C. *Langmuir* **2002**, *18*, 6484–6490.

(10) Bergström, L. M.; Kjellin, U. R. M.; Claesson, P. M. *J. Phys. Chem. B* **2004**, *108*, 1874–1881.

(11) Nizri, G.; Magdassi, S.; Schmidt, J.; Cohen, Y.; Talmon, Y. *Langmuir* **2004**, *20*, 4380–4385.

5773

dx.doi.org/10.1021/jp200486u |*J. Phys. Chem. B* 2011, 115, 5766–5774

(12) Nizri, G.; Lagerge, S.; Kamyshny, A.; Major, D. T.; Magdassi, S. *J. Colloid Interface Sci.* **2008**, *320*, 74–81.

(13) Berret, J. *J. Chem. Phys.* **2005**, *123*, 164703.

(14) Mészáros, R.; Varga, I.; Gilányi, T. *J. Phys. Chem. B* **2005**, *109*, 13538–13544.

(15) Trabelsi, S.; Raspaud, E.; Langevin, D. *Langmuir* **2007**, *23*, 10053–10062.

(16) Noskov, B. A.; Grigoriev, D. O.; Lin, S. Y.; Loglio, G.; Miller, R. *Langmuir* **2007**, *23*, 9641–9651.

(17) Ábrahám, Á.; Mezei, A.; Mészáros, R. *Soft Matter* **2009**, *5*, 3718–3726.

(18) Wu, Q.; Du, M.; Shangguan, Y.; Zhou, J.; Zheng, Q. *Colloids Surf., A* **2009**, *332*, 13–18.

(19) Binks, B. P. *Modern Characterization Methods of Surfactant Systems*; Marcel Dekker: New York, 1999.

(20) Kremer, F.; Schonhals, A. *Broadband Dielectric Spectroscopy*; Springer-Verlag: Berlin, 2002.

(21) Antonietti, M.; Maskos, M.; Kremer, F.; Blum, G. *Acta Polym.* **1996**, *47*, 460–465.

(22) D'Aprano, A.; Mesa, C. L.; Persi, L. *Langmuir* **1997**, *13*, 5876–5880.

(23) Bonincontro, A.; Michiotti, P.; Mesa, C. L. *J. Phys. Chem. B* **2003**, *107*, 14164–14170.

(24) Van Der Touw, F.; Mandel, M. *Biophys. Chem.* **1974**, *2*, 218–230. Van Der Touw, F.; Mandel, M. *Biophys. Chem.* **1974**, *2*, 231–241.

(25) Mandel, M.; Odijk, T. *Annu. Rev. Phys. Chem.* **1984**, *35*, 75–108.

(26) Mandel, M. *Biophys. Chem.* **2000**, *85*, 125–139.

(27) Ito, K.; Yagi, A.; Ookubo, N.; Hayakawa, R. *Macromolecules* **1990**, *23*, 857–862.

(28) Bordi, F.; Cametti, C.; Paradossi, G. *J. Phys. Chem.* **1995**, *99*, 274–284.

(29) Bordi, F.; Cametti, C.; Colby, R. H. *J. Phys.: Condens. Matter* **2004**, *16*, R1423–R1463.

(30) Bordi, F.; Cametti, C.; Gili, T.; Sennato, S.; Zuzzi, S.; Dou, S.; Colby, R. H. *Phys. Rev. E* **2005**, *72*, 031806.

(31) Bordi, F.; Cametti, C.; Sennato, S.; Zuzzi, S.; Dou, S.; Colby, R. H. *Phys. Chem. Chem. Phys.* **2006**, *8*, 3653–3658.

(32) Truzzolillo, D.; Cametti, C.; Sennato, S. *Phys. Chem. Chem. Phys.* **2009**, *11*, 1780–1786.

(33) Lian, Y.; Zhao, K.; Yang, L. *Phys. Chem. Chem. Phys.* **2010**, *12*, 6732–6741.

(34) Grosse, C. *J. Phys. Chem.* **1988**, *92*, 3905–3910.

(35) Baar, C.; Buchner, R.; Kunz, W. *J. Phys. Chem. B* **2001**, *105*, 2914–2922.

(36) Buchner, R.; Baar, C.; Fernandez, P.; Schrödle, S.; Kunz, W. *J. Mol. Liq.* **2005**, *118*, 179–187.

(37) Hardy, L. C.; Shriver, D. F. *Macromolecules* **1984**, *17*, 975–977.

(38) Hardy, L. C.; Shriver, D. F. *J. Am. Chem. Soc.* **1985**, *107*, 3823–3828.

(39) Király, Z.; Dekány, I. *J. Colloid Interface Sci.* **2001**, *242*, 214–219.

(40) Blanco-López, M.; Lobo-Castañón, M.; Ordieres, A. J. M.; Tuñón-Blanco, P. *Electroanalysis* **2007**, *19*, 207–213.

(41) Schwan, H. P. Determination of Biological Impedance. In *Physical Techniques in Biological Research*; Nastuk, W. L., Ed.; Academic Press: New York, 1963; Vol. 6, pp 323−406.

(42) Asami, K. *Langmuir* **2005**, *21*, 9032–9037.

(43) Steeman, P. A. M.; Turnhout, J. *Macromolecules* **1994**, *27*, 5421–5427.

(44) Wübbenhorst, M.; Turnhout, J. *J. Non-Cryst. Solids* **2002**, *305*, 40–49.

(45) Dobrynin, A. C.; Rubinstein, M. *Prog. Polym. Sci.* **2005**, *30*, 1049–1118.

(46) Lindman, B.; Brun, B. *J. Colloid Interface Sci.* **1973**, *42*, 388–399.

(47) Zettl, H.; Portnoy, Y.; Gottlieb, M.; Krausch, G. *J. Phys. Chem. B* **2005**, *109*, 13397–13401.

(48) Barnadas-Rodriguez, R.; Esterlich, J. *J. Phys. Chem. B* **2009**, *113*, 1972–1982.

(49) Mackie, A. D.; Panagiotopoulos, A. Z.; Szleifer, I. *Langmuir* **1997**, *13*, 5022–5031.

(50) Hadgiivanova, R.; Diamant, H. *J. Chem. Phys.* **2009**, *130*, 114901. Hadgiivanova, R.; Diamant, H. *J. Phys. Chem. B* **2007**, *111*, 8854–8859.

(51) Böhme, U.; Scheler, U. *Adv. Colloid Interface Sci.* **2010**, *158*, 63–67.

(52) Dukhin, S. S.; Shilov, V. N. *Dielectric Phenomena and the Double Layer in Disperse Systems and Polyelectrolytes*; Wiley: New York, 1974.

(53) Blum, G.; Maier, H.; Sauer, F.; Schwan, H. P. *J. Phys. Chem.* **1995**, *99*, 780–789.